Catal Lett (2008) 124:178–184
DOI 10.1007/s10562-008-9483-8

Physicochemical Characterization and H_2-TPD Study of Alumina Supported Ruthenium Catalysts

Bingyu Lin · Rong Wang · Xiujin Yu · Jianxin Lin ·
Feng Xie · Kemei Wei

Received: 31 January 2008 / Accepted: 24 March 2008 / Published online: 10 April 2008

Abstract A series of alumina supported ruthenium catalysts, which prepared by hydrogen treatment or hydrazine reduction, were characterized by N_2 adsorption, X-ray diffraction (XRD), X-ray fluorescence (XRF), CO chemisorption, and Temperature-programmed desorption of hydrogen (H_2-TPD). In contrast to the samples with conventional hydrogen reduction, there was almost no residual chlorine in the samples using $RuCl_3$ as precursor with hydrazine treatment. Furthermore, the dissolved aluminum could be removed much more easily in basic solution, which led to the higher BET surface and pore volume of hydrazine-reduction catalysts. Therefore, the active phase (Ru metal) would not be contaminated. Three main peaks, which occurred at about 150, 375, and 650 °C, respectively, were observed in the H_2-TPD profiles of Ru/Al_2O_3 catalysts with a high amount of residual chlorine. A new peak of desorption hydrogen centering at 240 °C, which was completely suppressed by the high amount of residual chlorine, might appear in the profiles of the samples with the washing procedure following hydrogen reduction or hydrazine treatment. The peaks with the desorption temperature lower than 500 °C were relative with dissociatively adsorbed hydrogen and spillover hydrogen simultaneity, and the peak at above 500 °C was caused by spillover hydrogen and would be stabilized by hydroxyl groups on alumina surface.

Keywords Hydrazine reduction · H_2-TPD · Chlorine · Ru/Al_2O_3

B. Lin · R. Wang (✉) · X. Yu · J. Lin · F. Xie · K. Wei
National Engineering Research Center of Chemical Fertilizer
Catalyst, Fuzhou University, 523 Gongye Road, Fuzhou,
Fujian 35002, P.R. China
e-mail: rwang@fzu.edu.cn

1 Introduction

Oxides supported ruthenium catalysts have been used in various catalytic reactions, such as the hydrogenolysis of paraffins and olefins [1, 2], isomerization of linoleic acid [3], selective hydrogenation of benzene [4, 5], Fischer-Tropsch synthesis [6–8] and ammonia synthesis [9–18]. Generally, $Ru_3(CO)_{12}$ or other chlorine-free ruthenium compounds rather than the stable and cheap $RuCl_3$ are employed as ruthenium precursor since the catalytic activity usually significantly decreased due to the presence of chlorine. For instance, Iyagba et al. [6] and Ragaini et al. [8] reported that the presence of chloride decreased significantly the CO hydrogenation activity of silica or alumina supported ruthenium catalyst as a result of a decrease in the number of reactive surface sites. Bernas and coworkers [3] suggested the acidic properties of residual chloride led to the lower selectivity to the desired CLA isomers. As for ammonia synthesis, chlorine suppresses the activity has been observed at ruthenium catalysts with different supports such as MgO, Al_2O_3 [9, 11, 17, 18]. The exact reason is still not fully understood, but two main ideas about it have been widely accepted. One is that some sites available for hydrogen adsorption are activated by chlorine [19, 20], thus the nitrogen activation and the catalytic activity are retarded. The other opinion on this is that the high electronegative chlorine atoms decrease the electron density at nearby surface ruthenium atoms and then prevents the triple $N{\equiv}N$ bond from rupturing [18, 21].

Many efforts have been done to decrease the amount of chlorine remained on the oxides supported ruthenium catalysts for enhancing the catalytic activity. Increasing the temperatures of hydrogen reduction is one of the common methods for eliminating residual chlorine. Both hydrogen adsorption and ammonia synthesis activity of $RuCl_3/MgO$ [9]

and $RuCl_3/Al_2O_3$ [15] have been observed to increase with increasing treatment temperature up to 627 °C as a result of the chlorine removal from the catalyst. However, chlorine still could be detected in Ru/MgO [9] or Ru/Al_2O_3 [22] even the hydrogen treatment temperature was high as 700 °C, which led to the severe sintering of the ruthenium particles. Washing the reduced samples with distilled water or aqueous ammonia was another effective method to remove chlorine [5, 6, 22, 23]. However, numbers of studies [5, 6, 23] demonstrated that complete chlorine removal was impossible to achieve by a washing procedure following hydrogen reduction.

Chemical reduction of metal salts dissolved in appropriate solvents is one of the methods for preparing metal nanoparticles powders, a variety of reducing agents including of alcohols, glycols and certain specialized reagents such as Tetrakis(hydroxymethyl) phosphonium chloride have been employed [24]. This reduction method has been successfully applied to obtain supported metal catalysts with nanoparticles and the support materials could act as a stabilizer for preventing the nanoparticles from agglomerating [25, 26]. Recently, Silica-supported nickel metal nanoparticles, which show more active in benzene hydrogenation than a conventional catalyst, have been successfully prepared by reduction of nickel acetate with hydrazine in aqueous medium [27–29]. Miyazaki et al. [13], Wu et al. [30], and Seetharamulu et al. [31] have respectively prepared the Al_2O_3, MgO, and Mg–Al hydrotalcite supported ruthenium catalysts by polyol reduction method using ethylene glycol as solvent. They found the polyol reduction catalysts showed excellent properties such as high dispersion of Ru, optimal ruthenium particle size and less residual chlorine, thus the higher activities for ammonia synthesis could be obtained.

Previously, a chlorine-free Sm–Ru/Al_2O_3 was prepared by hydrazine reduction base on $RuCl_3$, which showed much higher activity for ammonia synthesis than those obtained by conventional hydrogen treatment [32]. However, the previous result showed that the differences of the morphology and size of ruthenium particles were both slight, therefore, chlorine was suggested to be the key factor influencing on the activities of ruthenium catalysts. In this paper we concentrated on the studies of composition, physicochemical properties and H_2-TPD of Ru/Al_2O_3 samples obtained by hydrogen treatment and hydrazine reduction to learn more about the effect of reduction methods, the effect of chlorine on hydrogen adsorption of ruthenium catalysts also was discussed.

2 Experimental

2.1 Catalyst Preparation

Ru/Al_2O_3 catalysts were prepared according to Ref. [32], briefly, γ-Al_2O_3 (WHA219, obtained from Wenzhou Alumina Plant, China.) was crushed to 12–16 meshes, baked at 500 °C for 3 h and then impregnated with $RuCl_3$ aqueous solution. 3 g $RuCl_3/Al_2O_3$ samples were stirred for 10 min at room temperature in 0.1 mol/L KOH solutions (100 mL) with hydrazine, and the mole ratio of hydrazine to Ru was 3. After slowly heated up to 80–90 °C and maintained for 10 min, the as-prepared samples were filtered, washed with distilled water until neutrality and the Cl^- was not detected in washing solution ($AgNO_3$ test), the sample was denoted as Ru/Al_2O_3(h). Ru/Al_2O_3(H) was obtained by hydrogen reducing of $RuCl_3/Al_2O_3$ at 450 °C for 4 h, Ru/Al_2O_3(H) was further washed with distilled water until the disappearance of chlorine in the washing solution and labeled as Ru/Al_2O_3(H+W). For comparison, a Ru(h-Cl)/Al_2O_3 catalyst also was prepared, that is, 4.2 wt% HCl was introduced to Ru/Al_2O_3(h) by impregnation of HCl solution and then hydrogen reduction of the sample at 450 °C for 4 h, the weight ratios of Ru to Al_2O_3 were ca. 4 wt%.

2.2 Catalysts Characterization

The composition concentrations of catalyst were determined using a PANalytical Axios X-ray fluorescence spectrometer with a rhodium tube as the source of radiation. The samples were crushed and prepared to 30 mm diameter pressed pellets for analyzing. The results were analyzed by IQ+ and the concentrations were normalized to 100%.

X-ray diffraction (XRD) analysis was carried out on a PANalytical X' pert Pro diffractometer with uses CuKα radiation and works at 40 kV, 40 mA.

BET surface areas were measured by N_2 adsorption at −196 °C using Micromeritics ASAP 2020 instrument. The adsorption isotherm data were used to calculate the surface area of each sample via the Brunauer, Emmett and Teller (BET) equation.

Temperature-programmed desorption of hydrogen (H_2-TPD) experiment was carried out in a Micromeritics Autocue 2910 instrument. The sample (0.12 g) was packed into a reactor with quartz tubing, and was treated at 500 °C for 2 h under a flow of hydrogen (flow rate of 50 mL/min) without additional note. After cooled down to room temperature, the catalyst was purged in flow of argon (Linde, 99.999% purity; flow 30 mL/min) at for 1 h. The H_2-TPD experiment was performed by sample heating at a rate of 10 °C/min from room temperature to 850 °C under an argon flow (20 mL/min). The amount of desorbed hydrogen was measured by a TCD detector. All TPD experiments were performed at least in duplicate, with the datasets presented here being representative of the trends observed in each case.

Metal dispersion was measured by CO chemisorption using the apparatus described above for TPD experiments.

The catalyst was reduced at 500 °C for 2 h and then flushed with a helium stream for 1 h to remove H_2 adsorbed on the catalyst. After cooling down to room temperature in He, CO was injected at regular intervals until the area of the recorded peaks became constant. Based on a CO:Ru stoichiometry of 1 [33], Ru dispersion was calculated from the cumulative volume of CO adsorbed during pulse chemisorption [34] and the size of the ruthenium particle was estimated from the equation proposed by Borodzinski and Bonarowska [35].

3 Results and Discussion

3.1 XRF Analysis

Table 1 shows the composition concentrations of the alumina supported ruthenium catalysts, all metals were expressed as oxides. The chlorine content decreases significantly if the catalysts have been reduced in hydrogen for 4 h, however, the amount of the residual chlorine is quite high. The chlorine content changes slightly even the hydrogen treatment time is prolonged to 12 h, indicating that the amount of chlorine would not further decrease if the catalysts have been reduced in hydrogen for 4 h. In addition to high temperature reduction, which would lead to the severe sintering of the ruthenium particles [9, 22], washing the reduced samples with distilled water or aqueous ammonia is another effective method to eliminate chlorine [5, 6, 22, 23]. However, Table 1 also shows that complete chlorine removal is impossible to achieve by a washing procedure following hydrogen reduction, which is good accordance with other studies [5, 6, 23]. The reason is might be due to some strongly bound chlorides cannot be removed by a washing process after high-temperature treatment in hydrogen gas. According to Mazzueri et al. [5], the hydrogen-reduced $RuCl_3/Al_2O_3$ catalysts contained different Ru species such as Ru^0, ruthenium oxide, $RuCl_3$, and ruthenium oxychloride, washing the Ru/Al_2O_3 catalyst following hydrogen reduction at 400 °C for 6 h with 10% NH_4OH could remove the unreduced $RuCl_3$, but fail to eliminate ruthenium oxychloride.

In contrast, the amount chlorine detected by XRF in the catalyst with hydrazine reduction is very low. This can be easily comprehended considering hydrazine reduction takes place in a basic aqueous medium, then most chlorides generated during the reduction exist in solution and bind weakly with the support and Ru, and thus these chlorides could be removed by a washing process. The amount of chlorine in Ru/Al_2O_3(h-Cl), obtained by impregnating Ru/Al_2O_3(h) with HCl solution and then reducing in hydrogen for 4 h, is still quite large.

Table 1 Compositions concentrations (%) of the samples

Sample	Al_2O_3	Fe_2O_3	SiO_2	CaO	RuO_2	Cl
Al_2O_3	99.82	0.08	0.04	0.06	–[a]	–
Ru/Al_2O_3[b]	94.65	0.04	0.09	0.08	2.31	2.83
Ru/Al_2O_3(H)	96.72	0.05	0.07	0.08	2.14	0.94
Ru/Al_2O_3(12H)[c]	96.76	0.05	0.09	0.06	2.12	0.92
Ru/Al_2O_3(H+W)	97.00	0.09	0.08	0.06	2.37	0.40
Ru/Al_2O_3(h)	96.99	0.05	0.22	0.16	2.56	0.02
Ru/Al_2O_3(h-Cl)[d]	96.69	0.06	0.10	0.12	2.19	0.84

[a] No detected

[b] Unreduced catalyst

[c] Hydrogen reducing of $RuCl_3/Al_2O_3$ at 450 °C for 12 h

[d] Impregnation of Ru(h) with HCl and reduced in hydrogen

3.2 Physicochemical Characterization

Table 2 lists the measured surface areas of various catalysts. The surface area of Al_2O_3 is 210.2 m^2/g, after impregnating of Al_2O_3 by $RuCl_3$ aqueous solution followed by hydrogen treatment at 450 °C, the surface area of the material decreases to 177.2 m^2/g, and the pore volume also decreases from 0.562 to 0.489 cm^3/g. It is well known that the pH of $RuCl_3$ solution is low (in the range of 1–3) [22, 36], thus alumina would dissolve by the following reaction during impregnation [36]:

$$\begin{aligned} Al_2O_3(s) + 3HO(+) &\rightarrow 2Al(OH)_3 + 3H(+) \\ &\leftrightarrow 2A1^{3+} + 3H_2O + 3OH^- \end{aligned} \quad (1)$$

and alumina dissolution facilitates generations of adsorption sites, which would be benefit for the incorporation of Ru^{3+} and Cl^- into Al_2O_3 lattice, consequently, the well-dispersion Al_2O_3-supported ruthenium catalyst could be obtained and some strongly bound chlorides also appeared, however, some pores of Al_2O_3 are plugged by these dissolved alumina salt or chlorides generated during the preparation of metal supported catalysts, thus the surface area significantly decreases and ruthenium metal is

Table 2 Surface area, dispersion, and particle size of ruthenium

Samples	Surface area (m^2/g)	$V_{total\ pore}$ (cm^3/g)	FE[a]	d (nm)
Al_2O_3	210.0	0.562	–	–
Ru/Al_2O_3(H)	177.2	0.489	0.466	2.3
Ru/Al_2O_3(H+W)	180.1	0.498	0.484	2.2
Ru/Al_2O_3(h)	201.1	0.549	0.512	2.0
Ru/Al_2O_3(h-Cl)	177.1	–	0.503	2.1
Ru/Al_2O_3(12H)	174.4	–	0.454	2.4

[a] Ruthenium dispersion (fraction exposed, FE) was measured by CO chemisorption

contaminated. It should be rather difficulty to remove the dissolved aluminum by hydrogen treatment at high temperature since these aluminum species would react with chlorine.

Washing the hydrogen-reduced catalyst could remove some residual chlorine and the dissolved aluminum, therefore, the surface area and the pore volume both slightly increase.

Hydrazine reduction takes place in a basic aqueous medium, Al^{3+} is transformed to $Al(OH)_3$ at high pH ($pH > 9$) [37] or dissolve in basic aqueous. In such a way, the dissolved alumina is easily eliminated by generation of $Al(OH)_3$ and then Al_2O_3 formed by dehydration of $Al(OH)_3$ at high temperature, thus the surface area increases and some pores recover (Table 2 and Fig. 1), therefore, the active phase (Ru metal) is not contaminated by the dissolved aluminum or chlorine ions.

Table 2 also presents the Ru dispersion and ruthenium particle size obtained by CO chemisorption, the data show that the metal particle size of all samples in the range of 2.0–2.5 nm, indicating that the influence of the particle size could be excluded.

Figure 2 shows the XRD patterns of various samples, the reflections peaks corresponding to γ-Al_2O_3 are clearly observed in all XRD patterns of the samples (PDF 47-1308), and however, there are no reflections of ruthenium compounds, which might be as a result of the well dispersion of ruthenium compounds or the low Ru loading.

3.3 H_2-TPD

Thermal desorption curves of hydrogen from the various samples are presented in Figs. 3–5. The H_2-TPD profiles of supported ruthenium catalysts, which are good consistent with those of other transition metal catalysts such as Ni, Pt, Rh catalysts [38, 39], comprise three or more peaks owing to the formation of various active sites or the effect of spillover hydrogen. The profiles of Ru/Al_2O_3(H), Ru/

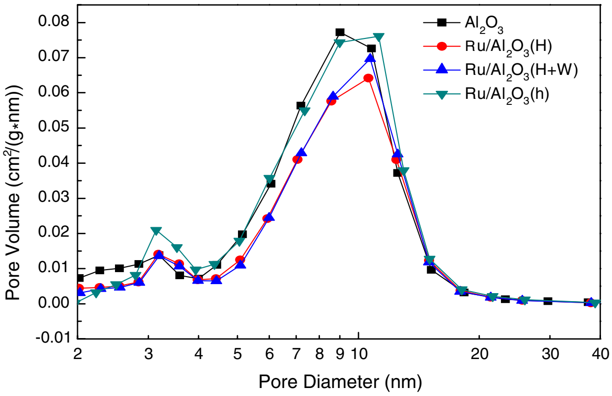

Fig. 1 Pore size distribution of various Ru/Al_2O_3 samples

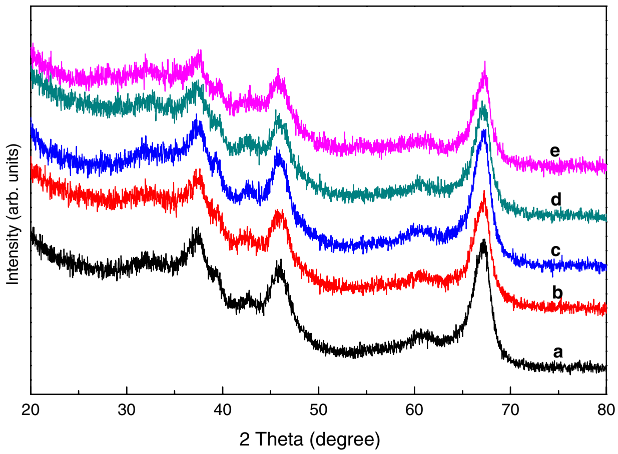

Fig. 2 XRD patterns of the samples: (a) Al_2O_3; (b) Ru/Al_2O_3(H); (c) Ru/Al_2O_3(H+W); (d) Ru/Al_2O_3(h); (e) Ru/Al_2O_3(h-Cl)

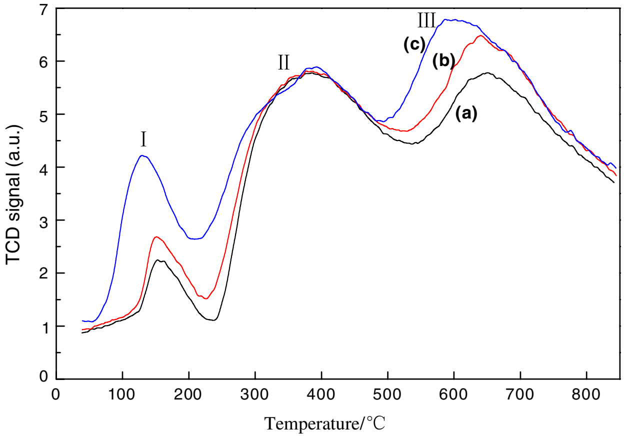

Fig. 3 H_2-TPD profiles of the ruthenium catalysts (a) Ru/Al_2O_3(H), (b) Ru/Al_2O_3(12H), (c) Ru/Al_2O_3(h-Cl)

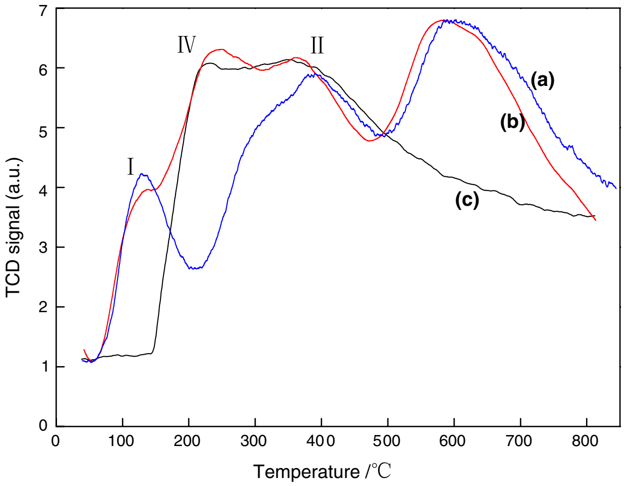

Fig. 4 H_2-TPD profiles of (a) Ru/Al_2O_3(h-Cl), (b) Ru/Al_2O_3(H+W), and (c) following the first TPD, Ru/Al_2O_3(H+W) was rereduced at 500 °C for 1 h, cooled in H_2 and then second TPD was carried out

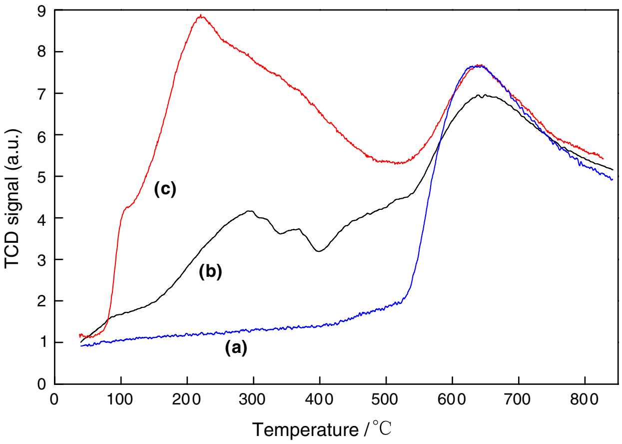

Fig. 5 H_2-TPD profiles of Ru/Al_2O_3(h) (a) reduced at 500 °C, flushed with Ar at 500 °C for 1 h and then cooled down to room temperature in Ar, (b) H_2-TPD after hydrogen pulse chemisorption, (c) hydrogen treatment at 500 °C for 2 h and then cooled down to room temperature in H_2

Al_2O_3(12H), and Ru/Al_2O_3(h-Cl) (Fig. 3) all show a sharp peak (peak I) in the temperature range of 40–200 °C, and the peak areas increase with the decrease of the chlorine content. Other two broad peaks appear at about 375 °C (peak II) and at above 500 °C (peak III) in the H_2-TPD profiles of all ruthenium catalysts.

In case of Ru/Al_2O_3(H+W) and Ru/Al_2O_3(h), in addition to the peaks at above 500 °C (peak III), only a broad, overlapping peak would be observed. It is worth noted that the overlapping peak shows the almost same onset temperature and endset temperature as those of the peak I and peak II on the profiles of the Ru/Al_2O_3 catalysts with hydrogen reduction, respectively. Furthermore, comparing the H_2-TPD profiles of Ru/Al_2O_3(H+W) with that of Ru/Al_2O_3(h-Cl) (Fig. 4), one can see that peak I and peak II also appear in the profiles of Ru/Al_2O_3(H+W). Thus it is responsible to assume that the hydrogen corresponding to peak IV arise, and then the broad peak appears in the profiles of Ru/Al_2O_3(H+W) and Ru/Al_2O_3(h) due to the peak IV is overlapped with peak I and peak II. The above-mentioned result also suggests that chlorine remarkably suppresses the hydrogen corresponding to peak IV centering at 240 °C, similar result that the residual chloride significantly suppressed the capacity for hydrogen adsorption also has been observed by other [22, 40].

Previously, Miller et al. [41, 42] studied hydrogen temperature-programmed desorption of various supported platinum catalysts such as Pt/Al_2O_3, Pt–K/LTL, $Pt–SiO_2$ after hydrogen reduction at 300, 450, or 650 °C and attributed only the reversible desorption occurred at approximately 175 °C to chemisorbed hydrogen. However, other different conclusion also was obtained by researchers. Kramer and Andre [43] studied the adsorption of hydrogen on alumina and Pt/Al_2O_3 by temperature-programmed desorption and suggested that the peak within the range of 50–400 °C mainly was caused by hydrogen dissociatively adsorbed on the platinum, which was in agreement with experiments on unsupported platinum [44, 45]. Menon and Froment [46, 47] also presented that the hydrogen with desorption temperature at about 250 °C should be a consequence of the stronger chemisorption of H_2 on Pt in $Pt–Al_2O_3$ or in platinum black. The hydrogen uptake obtained from hydrogen pulse chemisorption of Ru/Al_2O_3(h) at room temperature before H_2-TPD analysis is about 75 μmol/g, and the corresponding particle size is about 2.8 nm, which is close to the data obtained from CO pulse chemisorption (Table 2). Furthermore, there are several desorption peaks of hydrogen with the desorption temperature from room temperature to 500 °C in the TPD profile of Ru/Al_2O_3(h) with hydrogen pulse chemisorption (Fig. 5b). In contrast, there are no peaks with desorption temperature between 40 and 500 °C in the H_2-TPD profiles of Ru/Al_2O_3(h), which has been reduced at 500 °C and flushed with Ar at high temperature (Fig. 5a). The above-mentioned result shows that all H_2 with desorption temperature lower than 500 °C should be considered for calculating the dispersion of Ru/Al_2O_3 catalysts during pulse chemisorption. Very recently, Okal et al. [48] studied Ru dispersion in Ru/γ-Al_2O_3 catalysts by volumetric H_2 chemisorption at different temperatures (20–200 °C) and also observed a rather large amount of the irreversibly desorbed H_2. Therefore, the idea that the desorption peaks of hydrogen within the range of 30–500 °C all are relative with hydrogen dissociatively adsorbed on the ruthenium might be more reasonable for our Ru/Al_2O_3.

From Fig. 5, within the temperature range from room temperature to 500 °C, the peaks areas in the TPD profile of Ru/Al_2O_3(h) with hydrogen treatment at 500 °C for 2 h are higher than those with pulse chemisorption, indicating that there is also a large amount of spillover hydrogen. To further elucidate the problem, a reference should be given to the paper of Conner and Falconer [49], who have shown that hydrogen spillover always comprises of various steps, that is, adsorption and activation of a diatomic molecule onto a surface, the adsorbed species move across the surface to the interface with the second surface, then diffuse and spillover on to the nonadsorbing surface. Similar fast and slow adsorption of H_2 also has been observed over Rh/Al_2O_3 catalysts. Crucq et al. [50, 51] found that when Rh/Al_2O_3 catalysts were adsorbed H_2, some hydrogen would be completely adsorbed within several minutes and other would not stop even more than 20 h at low temperature. Moreover, the high absorbed temperature would decrease the time and the corresponding adsorbed hydrogen amount of slow adsorption [50, 51]. As for our Ru/Al_2O_3 catalysts, it could be reasonable to assume that the diffuseness rate at room temperature after pulse chemisorption is much less than that of adsorption and activation of a diatomic molecule onto a surface, therefore, it would be considered by instrument that hydrogen adsorption has been complete, in fact, hydrogen spillover would continuously occur. Hydrogen treatment before H_2-TPD is carried out at high temperature and the time is much longer, then hydrogen spillover is more complete, thus the adsorbed hydrogen uptakes also are much higher.

Only the peak at above 500 °C is observed in the profile of the Ru/Al_2O_3(h) (Fig. 5a), which has been reduced at 500 °C, flushed with Ar at 500 °C for 1 h and then cooled down to room temperature in Ar, indicating that the high-temperature peak is caused by hydrogen remained on the sample during high temperature reduction. However, if the sample is immediately cooled to 500 °C and reexposed to H_2 for 1 h after the first TPD has been achieved, then cooled in flowing H_2 to room temperature and a second TPD is carried out (Fig. 4b), the high-temperature peak would disappear. This result confirms that the high-temperature peak of hydrogen desorption is likely due to spillover hydrogen located at support and would change if the structure of the support varies, which is good accordance with the result over Pt catalysts. According to Altham and Webb [52], hydroxyl groups were necessary to keep the stabilization of spillover hydrogen over Pt catalysts supported on alumina and silica. In such a case, high irreversible dehydroxylation of the alumina with high temperature treatment leads to the instability of spillover hydrogen. The peak at about 120 °C also disappears in the second TPD profile, which might be due to some Ru metal particles are sintered at high temperature.

Combining the results of Figs. 3–5, one can see that peak II at about 375 °C and peak III at above 500 °C both are almost independence of residual chlorine. Obviously, these peaks are dominated by spillover hydrogen under the conditions of high temperature treatment with hydrogen for 2 h. In contrast, the adsorbed hydrogen corresponding to desorption temperatures are lower than 300 °C, is remarkably suppressed by chlorine remained on alumina supported ruthenium catalysts, especially the peak centering at above 240 °C almost completely disappear. The hydrogen with desorption temperature lower than 500 °C is comprised of chemisorption hydrogen and spillover hydrogen simultaneity. It seems that more than four kinds of active sites for hydrogen spillover appear on Ru/Al_2O_3 surface, which might be as a result of complex surface chemistry of alumina containing aluminum ions, oxide ions and hydroxyl ions with random defects [53, 54]. Therefore, further studies for understanding the exact hydrogen species and distinguishing the exact contents of various hydrogen species are necessary.

As for ammonia synthesis, some sites available for hydrogen adsorption are contaminated by chlorine, thus the nitrogen activation and the catalytic activity are retarded as a consequent of the competitive adsorption between hydrogen and nitrogen on the active sites of ruthenium catalysts [17, 55–57], furthermore, the results of H_2-TPD study show the amount of spillover hydrogen is rather large, and it is clear that some spillover hydrogen would be not benefit for ammonia synthesis since the reaction temperature of ammonia synthesis is usually lower than 475 °C. Consequently, promoters, which always are used for enhancing the catalytic activity [10, 12, 13], not only act as scavengers by reacting with Cl^- or electron donors to the ruthenium surface or decrease the acidity of alumina, but also act as the promoters for reducing the amount of spillover hydrogen. That might be the reason why lanthanide compounds can increase the activities of ruthenium catalysts. Extensive studies for further understanding the effect of spillover hydrogen on the ammonia synthesis activities of Ru/Al_2O_3 catalysts are in progress.

4 Conclusions

Rather high chlorine content remained on Ru/Al_2O_3 catalysts prepared using $RuCl_3$ as precursor and subjected to hydrogen reduction, washing the reduced samples with distilled water or prolonging the reduction time could not remove residual chlorine completely. In contrast, most chlorine could be easily eliminated by hydrazine reduction in basic solution. Furthermore, hydrazine reduction method significantly overcomes the disadvantage effect of the dissolved alumina salt or chlorides on the pores plug of Al_2O_3, and then the active phase (Ru metal) would not be contaminated.

Three main peaks, which occurred at about 150, 375, and 650 °C, respectively, are observed in the H_2-TPD profiles of Ru/Al_2O_3 catalysts with only hydrogen treatment. A new peak of desorption hydrogen centering at 240 °C, which was completely suppressed by the high amount of residual chlorine, appeared in the profiles of the Ru/Al_2O_3(H+W) or Ru/Al_2O_3(h) samples. Some hydrogen with the desorption temperature with from room temperature to 500 °C is caused by hydrogen dissociatively adsorbed on the ruthenium simultaneity, and other large amount of hydrogen with the same desorption temperature range is relative with spillover hydrogen. The hydrogen desorption peaks at above 500 °C were caused by spillover hydrogen located at support, which were stabilized by hydroxyl groups on alumina surface.

Acknowledgments This study was supported by the National Natural Science Foundation of China (20576021), Science & Technology Priority Project of Fujian Province (2005HZ01-2) and National Key Technology R&D Program of China (2007BAE08B00).

References

1. Madon RJ, Reyes SC, Iglesia E (1991) J Phys Chem 95:7795
2. Sinfelt JH (1970) Catal Rev 3:175
3. Bernas A, Kumar N, Laukkanen P, Vayrynen J, Salmi T, Murzin DY (2004) Appl Catal A 267:121
4. Milone C, Neri G, Donato A, Musolino MG, Mercadante L (1996) J Catal 159:253
5. Mazzieri V, Coloma-Pascual F, Arcoya A, L'Argentiere PC, Figoli NS (2003) Appl Surf Sci 210:222
6. Iyagba ET, Eddy Hoost T, Nwalor JU, Goodwin JG (1990) J Catal 123:1
7. Reinikainen M, Niemela MK, Kakuta N, Suhonen S (1998) Appl Catal A 174:61
8. Ragaini V, Carli R, Bianchi CL, Lorenzetti D, Vergani G (1996) Appl Catal A 139:17
9. Murata S, Aika KI (1992) Appl Catal A 82:1
10. Murata S, Aika K (1992) J Catal 136:118
11. Moggi P, Albanesi G, Predieri G, Spoto G (1995) Appl Catal A 123:145
12. Kadowaki Y, Aika K (1996) J Catal 161:178
13. Miyazaki A, Balint L, Aika K, Nakano Y (2001) J Catal 204:364
14. Bielawa H, Hinrichsen O, Birkner A, Muhler M (2001) Angew Chem Int Ed 40:1061
15. Murata S, Aika K (1992) J Catal 136:110
16. Aika K, Takano T, Murata S (1992) J Catal 136:126
17. Rosowski F, Hornung A, Hinrichsen O, Herein D, Muhler M, Ertl G (1997) Appl Catal A 151:443
18. Shiflett WK, Dumesic JA (1981) Ind Eng Chem Fund 20:246
19. Lu K, Tatarchuk BJ (1987) J Catal 106:166
20. Lu K, Tatarchuk BJ (1987) J Catal 106:176
21. Zeng HS, Inazu K, Aika K (2001) Appl Catal A 219:235
22. Narita T, Miura H, Ohira M, Hondou H, Sugiyama K, Matsuda T, Gonzalez RD (1987) Appl Catal 32:185
23. Mieth JA, Schwarz JA (1989) J Catal 118:218
24. Rao CNR, Kulkarni GU, Thomas PJ, Edwards PP (2000) Chem Soc Rev 29:27
25. Toshima N, Teranishi T, Asanuma H, Saito Y (1992) J Phys Chem 96:3796
26. Brayner R, Viau G, da Cruz GM, Fievet-Vincent F, Fievet F, Bozon-Verduraz F (2000) Catal Today 57:187
27. Boudjahem AG, Monteverdi S, Mercy M, Ghanbaja D, Bettahar MM (2002) Catal Lett 84:115
28. Boudjahem AG, Monteverdi S, Mercy M, Bettahar MM (2004) Catal Lett 97:177
29. Boudjahem AG, Monteverdi S, Mercy M, Bettahar MM (2004) J Catal 221:325
30. Wu S, Chen JX, Zheng XF, Zeng HS, Zheng CM, Guan NJ (2003) Chem Commun:2488
31. Seetharamulu P, Kumar VS, Padmasri AH, Raju BD, Rao KSR (2007) J Mol Catal A: Chem 263:253
32. Lin B, Wang R, Lin J, Du S, Yu X, Wei K (2007) Catal Commun 8:1838
33. Liang CH, Wei ZB, Xin Q, Li C (2001) Appl Catal A 208:193
34. Webb PA, Orr C (1997) Analytical methods in fine particle technology. Micromeritics Instrument corp, Norcross, p 70
35. Borodzinski A, Bonarowska M (1997) Langmuir 13:5613
36. Mieth JA, Schwarz JA (1989) Appl Catal 55:137
37. Hua W, Xia Y, Yue Y, Gao Z (2000) J Catal 196:104
38. Paal Z, Menon PG (1983) Catal Rev 25:229
39. Falconer JL, Schwarz JA (1983) Catal Rev 25:141
40. Wu X, Gerstein BC, King TS (1992) J Catal 135:68
41. Miller JT, Meyers BL, Modica FS, Lane GS, Vaarkamp M, Koningsberger DC (1993) J Catal 143:395
42. Miller JT, Meyers BL, Barr MK, Modica FS, Koningsberger DC (1996) J Catal 159:41
43. Kramer R, Andre M (1979) J Catal 58:287
44. Tsuchiya S, Amenomiya Y, Cvetanovic RJ (1970) J Catal 19:245
45. Stephan JJ, Ponec V, Sachtler WMH (1975) J Catal 37:81
46. Menon PG, Froment GF (1981) Appl Catal 1:31
47. Menon PG, Froment GF (1979) J Catal 59:138
48. Okal J, Zawadzki M, Kepinski L, Krajczyk L, Tylus W (2007) Appl Catal A 319:202
49. Conner WC, Falconer JL (1995) Chem Rev 95:759
50. Crucq A, Degols L, Frennet A, Lienard G (1989) Catal Today 5:223
51. Crucq A, Degols L, Frennet A, Lienard G (1990) J Mol Catal 59:257
52. Altham JA, Webb G (1970) J Catal 18:133
53. Peri JB (1965) J Phys Chem 69:220
54. Peri JB, Hannan RB (1960) J Phys Chem 64:1526
55. Siporin SE, Davis RJ (2004) J Catal 222:315
56. Urabe K, Aika K-I, Ozaki A (1976) J Catal 42:197
57. Rambeau G, Amariglio H (1981) J Catal 72:1